Biodegradable Photocrosslinkable Poly(depsipeptide-*co*-ε-caprolactone) for Tissue Engineering: Synthesis, Characterization, and *In Vitro* Evaluation

Laura Elomaa,[1,2] Yunqing Kang,[1] Jukka V. Seppälä,[2] Yunzhi Yang[1,3]

[1]Department of Orthopaedic Surgery, Stanford University School of Medicine, 300 Pasteur Drive, Stanford, California 94305
[2]Department of Biotechnology and Chemical Technology, Aalto University School of Chemical Technology, Kemistintie 1, 02150 Espoo, Finland
[3]Department of Materials Science and Engineering, Stanford University School of Engineering, 300 Pasteur Drive, Stanford, California 94305
Correspondence to: Y. Yang (E-mail: ypyang@stanford.edu)

Received 9 July 2014; accepted 6 September 2014; published online 25 September 2014
DOI: 10.1002/pola.27400

ABSTRACT: Stereolithography has become increasingly popular in scaffold fabrication due to automation and well-controlled geometry complexity, and consequently, there is a great need for new suitable biodegradable photocrosslinkable polymers. In this study, a new type of photocrosslinkable poly(ester amide) was synthesized based on ε-caprolactone and L-alanine-derived depsipeptide and was applied to fabrication of three-dimensional (3D) scaffolds by stereolithography. ^{1}H nuclear magnetic resonance and Fourier transform infra-red analysis confirmed the formation of new bonds during the polymer synthesis. Incorporation of depsipeptide increased the glass transition temperature and hydrophilicity of the polymer and accelerated hydrolytic degradation compared with the poly(ε-caprolactone) homopolymer. The compressive strength of the 3D scaffolds increased with the increasing depsipeptide content. This work demonstrated that incorporation of depsipeptide into photocrosslinkable polyesters resulted in excellent cytocompatibility and tunable degradation rates and mechanical properties and thus expanded the repertoire of biomaterials suitable for 3D photofabrication of high-resolution tissue engineering scaffolds. © 2014 Wiley Periodicals, Inc. J. Polym. Sci., Part A: Polym. Chem. **2014**, *52*, 3307–3315

KEYWORDS: crosslinking; photopolymerization; poly(ester amide); ring-opening polymerization; stereolithography

INTRODUCTION Biodegradable photocrosslinkable polymers are an important group of biomaterials that can be processed with high resolution into three-dimensional (3D) tissue engineering scaffolds. The most widely used photocrosslinking-based additive manufacturing technology is stereolithography that allows for the preparation of highly porous scaffolds by following a computer-aided design file in a spatially and temporally controllable manner.[1] The mild reaction conditions and use of visible light make photocrosslinking feasible for scaffold fabrication even in the presence of living cells.[2] The constantly increasing use of photofabrication methods for preparing tissue engineering scaffolds is leading to a greater demand for biocompatible photocrosslinkable polymers. To date, a limited variety of biodegradable photocrosslinkable polymers has been synthesized, including polyanhydrides[3] and various polyesters based on polylactides,[4–6] poly(ε-caprolactone) (PCL),[7–9] poly(trimethylene carbonate),[10] and poly (propylene fumarate).[11]

Although photocrosslinkable aliphatic polyesters have tunable mechanical properties and they are sensitive to hydrolytic degradation, the lack of biological functionality limits their use in biomedical applications. In addition, acidic degradation products of polyesters may cause irritating side effects at high concentrations.[12] To overcome these limitations, the copolymerization of esters with ampholytic α-amino acids may provide a feasible approach for tailoring polymer properties. Amino acids are attractive building blocks due to their abundant availability and a large diversity of functional groups in their side chains.[13] Amino acids as degradation products are expected to be non-toxic and readily metabolized.[14]

Poly(ester amide)s combine the biological functionality of amino acids with the easily hydrolyzable groups of polyesters that ensure the polymer biodegradability.[15] Polydepsipeptides (PDPs), which are copolymers of α-hydroxy acids

Additional Supporting Information may be found in the online version of this article.

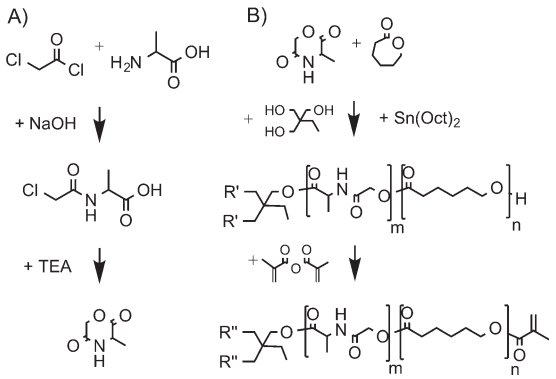

SCHEME 1 (**A**) The synthesis of the cyclic MMD monomer and (**B**) the ROP of the cyclic monomers followed by the methacrylation of the star-shaped hydroxyl-ended oligomers.

and α-amino acids, are an important class of the poly(ester amide)s.[16] PDPs can be synthesized via ring-opening polymerization (ROP) of morpholine-2,5-dione (MD) monomers, which are six-membered rings composed of a single α-amino acid and a single α-hydroxy acid residue.[17] The use of cyclic MD monomers allows for easy copolymerization with other cyclic monomers such as lactides and ε-caprolactone (CL).[18–21] Previously, triblock copolymers of leucine-derived PDP with poly(L-lactide) (PLLA) and poly(ethylene glycol) (PEG) have been studied for use as antiadhesive membranes,[22] and multiblock copolymers of various PDPs and PCL have shown stimuli-responsive behavior.[23] Triblock copolymers of alanine-derived PDP with PLLA and PEG have been used as micellar drug delivery systems.[24] However, all of these polymers have been thermoplastic, and only a very small effort has been put toward developing photocrosslinkable copolymers of PDPs. Previously, only photocrosslinkable copolymers of serine-derived depsipeptides have been synthesized by acrylating the hydroxyl groups of the serine side chains along the copolymers of depsipeptide and polyesters.[25]

In our study, we established a new synthesis scheme to create a photocrosslinkable poly(ester amide) platform based on CL and L-alanine as a model amino acid. By using an amino acid-derived depsipeptide as a comonomer, we intended to tailor the characteristics of the existing photocrosslinkable polyesters and thus expand their use in biomedical applications. In this study, the chemical, thermal, and degradation properties of the new materials were characterized, and their *in vitro* cytocompatibility was evaluated. The resulting photocrosslinkable copolymers were used to fabricate mathematically designed tissue engineering scaffolds by stereolithography, and the mechanical properties of the scaffolds were characterized.

EXPERIMENTAL

Materials

The CL monomer (Solvay Chemicals) was distilled under reduced pressure before polymerization. L-alanine (ICN Biomedicals), chloroacetyl chloride (Fluka), tin(II) 2-ethylhexanoate ($Sn(Oct)_2$), trimethylolpropane, methacrylic anhydride, and triethylamine (Sigma-Aldrich) were used as received. DL-camphorquinone (CQ, Acros Organics) and ethyl-4-dimethylaminobenzoate (EDMAB, TCI) were used as received. Lucirin® TPO-L and Orasol® Orange G were obtained from BASF. Phosphate buffered saline (PBS) was obtained from Life Technologies. Mouse pluripotent mesenchymal cells C3H10T1/2, Clone 8[26] were obtained from ATCC (ATCC® CCL-226™), and immortalized human-umbilical-vein endothelial cells (HUVECs) were a generous gift from the late Dr. J. Folkman, Children's Hospital, Boston. Dulbecco's modified Eagle's medium (DMEM), fetal bovine serum (FBS), antibiotic solution, and trypsin-ethylenediaminetetraacetic acid (EDTA) solution were purchased from Invitrogen Co. EBM™ endothelial basal medium containing a EGM™ Single Quots™ kit was purchased from Lonza Inc. 3-(4,5-Dimethyl-2-thiazolyl)-2,5-diphenyl-2H-tetrazolium bromide (MTT), *p*-nitrophenyl phosphate liquid substrate system, and Triton™ X-100 were purchased from Sigma-Aldrich, and Pico Green® dsDNA assay kit was obtained from Invitrogen Co.

Synthesis of a 3-Methyl-morpholine-2,5-dione (MMD) Monomer [Scheme 1(A)]

Cyclic MMD monomers were synthesized in a two-step reaction, starting with the reaction of an α-amino acid with chloroacetyl chloride followed by cyclization of the resulting intermediate chloroacetyl amino acid.[24,27] First, L-alanine (17.5 g, 0.20 mol) was dissolved in diethyl ether/water (1:1 v/v) mixture (75 mL) in a salt/ice bath (−5 °C), and the solution was mixed with aqueous 4 M NaOH solution (50 mL). Chloroacetyl chloride (25 g, 0.22 mol) was dissolved in diethyl ether (25 mL) and added dropwise to the amino acid solution simultaneously with aqueous 4 M NaOH solution (75 mL) over a 20-minute period under vigorous stirring. The pH of the mixture was held at 11 during the reaction. After the addition was complete, the aqueous layer was acidified to pH 1 with aqueous 4 M HCl and extracted three times with ethyl acetate. The combined organic layers were washed three times with saturated NaCl solution, dried with $MgSO_4$, and concentrated under vacuum. Yield 81%; mp 97 °C; ^{1}H NMR (D_20) $\delta = 1.33–1.34$ (d, 3H, CH_3), 4.05 (s, 2H, CH_2), 4.28–4.30 (q, 1H, CH).

Before beginning the cyclization step, a carefully dried flask and dropping funnel were evacuated and flushed 10 times with dry nitrogen. The white crystals of *N*-chloroacetyl-L-alanine (10 g, 0.06 mol) were dissolved in dry *N,N*-dimethylformamide (DMF, 50 mL) and added dropwise to a mixture of triethylamine (6.13 g, 0.06 mol) in DMF (200 mL) under vigorous stirring. The reaction was run at 90 °C for 8 h under a nitrogen atmosphere. After the reaction was complete, the solution was kept at room temperature overnight and the crystallized triethylamine-hydrochloride salt was filtered out of the solution. The solvent was removed at 30 °C under reduced pressure, and white MMD crystals were obtained after precipitation in chloroform and three recrystallizations

in diethyl ether. Yield 52%; mp 151 °C; ^{1}H NMR (D_20) $\delta = 1.39–1.41$ (d, 3H, CH_3), 4.30–4.34 (q, 1H, CH), 4.71–4.86 (2d, 2H, CH_2).

Synthesis of Photocrosslinkable Macromers [Scheme 1(B)]

Photocrosslinkable copolymers of MMD and CL were synthesized by a ROP reaction of the monomers and further methacrylation of the resulting hydroxyl-ended oligomers. Three different hydroxyl-ended oligomers with a targeted molecular weight of 750 g/mol were synthesized. The copolymers contained 5/95 mol% of MMD/CL (PDP5) and 10/90 mol% of MMD/CL (PDP10), and a PCL homopolymer (PCL) was used as a reference polymer. The appropriate amounts of the monomers (the amounts are listed in the supporting information) were added to the silanized and dried flask together with a trimethylolpropane initiator and 0.02 mol% of $Sn(Oct)_2$ as a catalyst. The flask was evacuated and flushed several times with dry nitrogen, and the reaction was run at 120 °C for 64 h. The resulting three-armed hydroxyl-ended oligomers were functionalized with a 100 mol% excess of methacrylic anhydride at 60 °C for 24 h. After methacrylation, the resulting macromers were precipitated several times in cold hexane and dried under reduced pressure. The yield of the macromers was around 95–97%.

Photocrosslinking of Polymer Films

To study the photocrosslinking characteristics and *in vitro* degradation of the new polymers, the methacrylated macromers were photocrosslinked into polymer films. First, the macromers were mixed with a photoinitiator solution containing 0.5 wt% of CQ and 0.5 wt% of EDMAB in a small amount of acetone. Acetone was allowed to evaporate and the polymers were photocrosslinked with a visible light projector (Vivitek) for 2 minute. Gel contents of the photocrosslinked polymers were measured by extracting the polymer samples in acetone for 24 h and drying overnight *in vacuo*. The gel content was obtained by dividing the dry weight of the samples after extraction by their dry weight before extraction.

Physiochemical Characterization

^{1}H nuclear magnetic resonance (NMR) spectra were recorded on a Bruker Avance-III 400 MHz spectrometer. A sample was dissolved in deuterium oxide or deuterated chloroform and its spectrum was acquired in a 5-mm NMR tube at room temperature. Gel permeation chromatography (GPC) samples were dissolved in tetrahydrofuran (THF) (5 mg/mL) and the analysis was run in THF at a flow rate of 1 mL/min. The chromatograph (Vistotek) was equipped with 5-μm Waters columns (300 mm × 7.7 mm) and a refractive index detector (Viscotek S3580), and the system was calibrated using monodisperse polystyrene standards (Polymer Laboratories). Thermal properties of the oligomers were determined using a Mettler Toledo Stare DSC 821^e differential scanning calorimeter (DSC). A sample was first heated from 25 °C to 100 °C at a rate of 20 °C/min, after which the temperature was decreased to −100 °C at 10 °C/min. After 2 minutes at −100 °C, the sample was heated from −100 °C to 100 °C at a rate of 10 °C/min. Melting points (T_m) and glass transition temperatures (T_g) were determined from the second heating scan. The amounts of peptide bonds and reacted double bonds of the macromers were determined using a Bruker Vertex 70 FTIR spectrometer with a diamond attenuated total reflection (ATR). Hydrophilicity of the photocrosslinked films was characterized by contact angle measurements with deionized water.

Degradation Study *In Vitro*

In vitro hydrolytic degradation of the photocrosslinked polymers was measured by following the mass loss of the unextracted photocrosslinked films ($d = 8$ mm, $h = 0.3$ mm, $n = 3$) in an aqueous environment. The samples were put in PBS (pH 7.4) at 37 °C with shaking at 150 rpm, and after a predetermined time, they were removed from the media and subsequently washed with deionized water and dried for 48 h *in vacuo*. The media was changed every 72 h during the degradation study.

Cell Cultures

C3H10T1/2 mouse mesenchymal cells on their tenth passage were cultured in basal medium consisting of DMEM with 10% FBS and 1% antibiotic solution. HUVECs were cultured in endothelial basal medium (EBM-2) with a Single Quots (EGM-2, excluding hydrocortisone) endothelial growth supplement, 10% FBS, and 1% antibiotic solution. All cells were cultured under standard conditions (5% CO_2, 37 °C, 95% humidity). Cells were subcultured using a 0.25% trypsin-EDTA solution. Polymer samples were sterilized with three immersions in 70% ethanol and further washed three times with PBS and dried in a sterile hood.

Cytocompatibility with HUVECs

The cytotoxicity of the photocrosslinked polymers was tested by measuring the metabolic activity of HUVECs on polymer films. About 76 μL of cell suspension containing 1×10^4 cells was added on the top of the photocrosslinked films ($d = 8$ mm, $h = 0.3$ mm, $n = 3$) and on a 24-well tissue culture polystyrene (TCPS) plate as a control. After the cell seeding, the samples were incubated for 30 minutes, after which fresh medium was added up to 1 mL. At time points of 1, 4, and 7 days, the metabolic activity of HUVECs was measured using a colorimetric MTT assay. Polymer films without cells were used to subtract the effect of the polymer itself on the color change. At the given time points, medium was removed and 500 μL of fresh serum-free medium and 50 μL of 5 mg/mL MTT in PBS were added into the wells. After incubation for 3 h, the medium was removed and the samples were shaken in 400 μL of dimethyl sulfoxide (DMSO) for 30 minutes. The optical density of the dissolved formazan crystals in 100 μL of DMSO aliquots was read using a microplate reader (TECAN) at 490 nm.

Proliferation and Differentation of Mouse Mesenchymal Cells

To study the suitability of the new polymers for bone tissue engineering, proliferation and osteogenic activity of

pluripotent C3H10T1/2 cells were monitored by measuring the amount of double-stranded DNA (dsDNA) and alkaline phosphatase (ALP) specific activity of the cells on the photocrosslinked films. Cells were seeded onto the polymer films with a density of 1×10^4 cells in 36 μL of medium. After seeding the cells, the films were incubated for 30 minutes, after which medium was added up to 1 mL. After 3, 7, and 14 days of cell culturing, the films were washed twice with PBS and preserved at -80 °C. After repeating a freeze/thaw cycle three consecutive times at -80 °C/37 °C, the samples were lysed in 500 μL of 0.2% Triton X-100 in PBS and homogenized by sonication for 30 seconds in an ice bath. The dsDNA content was measured using the Pico Green assay. About 50 μL of the working reagent was mixed with 50 μL of the cell lysate, and after 5 minutes, the samples were read using a fluorescence/chemiluminescence spectrophotometer (Biotek, Flx800) at 485/528 nm excitation/emission. The obtained values were compared with the standard DNA curve. The ALP activities of the same samples were measured using a colorimetric *p*-nitrophenyl phosphate (*p*-NPP) method, which is based on the conversion of the *p*-NPP substrate into p-nitrophenol (*p*-NP) in the presence of ALP, where the conversion rate is proportional to the ALP activity.[28] About 50 μL of the working solution was incubated with 50 μL of the cell lysate for 45 minutes at 37 °C, and the absorbance was read using a microplate reader (TECAN) at 405 nm. The results were compared with the standard *p*-NP curve.

Stereolithography of Porous Scaffolds and Characterization

Porous scaffolds were prepared using an EnvisionTEC Perfactory® Mini Multilens machine utilizing digital light processing technology. The gyroid pore architecture of the scaffolds was modeled using the free K3DSurf surface generator (k3dsurf.sourceforge.net). The stl-files were prepared using the Rhinoceros® software (McNeel). Scaffolds of 8.3 mm in diameter and 3 mm in height were built using a photocrosslinkable resin containing methacrylated macromer mixed with Lucirin® TPO-L photoinitiator (3 wt %) and Orasol Orange G dye (0.10 wt %). The layer thickness was 50 μm with an exposure time of 12 seconds and a light intensity of 1600 mW/dm^2. A lens with a focal distance of 85 mm was used. After fabrication, any uncured macromer was removed from the scaffolds by extraction with a mixture (1:1 v/v) of acetone and isopropanol. The scaffolds were dried *in vacuo* until a constant weight was achieved. To visualize the scaffold surface, the samples were sputtered with a gold/palladium alloy and observed with a scanning electron microscope (SEM, FEI XL30 Sirion) at 5 kV. Mechanical properties of the photocrosslinked scaffolds were measured using an Instron 5944 mechanical tester with a 2 kN load cell. A scaffold was placed between two parallel plates and compressed with a rate of 1% strain/second using a 1 N preload.

Statistical Analysis

For a statistical analysis, samples were always used in triplicate, and the statistical significance was determined with the IBM SPSS Statistics software using a one-way ANOVA followed by Tukey's *post hoc* test ($p < 0.05$).

RESULTS AND DISCUSSION

Synthesis of the Monomer, Oligomers, and Methacrylated Macromers

The cyclic MMD monomer was synthesized via a two-step reaction by first synthesizing chloroacetyl alanine that was then cyclized into a MMD monomer. Melting points of the resulting chloroacetyl alanine and MMD were 97 °C and 151 °C, respectively, which are comparable to the values published previously, 93 °C–96 °C for chloroacetyl alanine and 153.5 °C–154.5 °C for MMD.[27] The chemical structures of the synthesized materials were characterized with ^{1}H NMR. Formation of the cyclic MMD monomer was verified when the singlet peak *1* at 4.05 ppm [Fig. 1(A)] disappeared and two doublet peaks *1* at 4.70–4.86 ppm appeared [Fig. 1(B)]. The obtained MMD monomer was used to synthesize the star-shaped oligomers, which were further methacrylated to obtain photocrosslinkable macromers. The ROP of monomers resulted in peaks *a–h* and *1–3*, which are attributed to the protons of the star-shaped oligomer as assigned in Figure 1(C). No monomers were seen in the resulting ^{1}H NMR spectra, whereas a small peak *f′* attributed to the unreacted arms of TMP initiator was detected. Further end-capping the oligomer with methacrylic anhydride resulted in the peaks *i, j*, and *k*, which are attributed to the methacrylate end-groups of the resulting macromer, and the peak *a′* which is attributed to the protons of the last CL unit preceding the methacrylate group [Fig. 1(D)]. The methacrylation was continued until no peak *a′* of the oligomer, attributed to the protons next to the hydroxyl end-groups, was seen in the ^{1}H NMR spectra, indicating the degree of methacrylation to be close to 100%. The purity of the resulting photocrosslinkable macromers was ensured by precipitating the macromers with hexane until the excess of methacrylic anhydride peaks at around 2.04, 5.85, and 6.26 ppm were removed. The integrals of the small peaks observed near the peaks *i, j, and k* in Figure 1(D) were not decreased by purification and are attributed to the methacrylate end-groups of the previously unreacted initiator arms that are typical to low-molecular weight star-shaped polymers.

The molecular weights of the oligomers were calculated using the ^{1}H NMR integration. The average number of MMD and CL units per oligomer was determined by comparing the integral of the peak *h* attributed to the TMP initiator with the integrals of the peaks *1* and *2* attributed to the MMD units and the peak *e* attributed to the CL units (the integrals are shown in the Supporting Information). The increase in the amount of depsipeptide was seen as an increase in the integral of the peaks *1* and *2* and as a decrease in the integral of the peak *e*. Table 1 shows the calculated molecular weights of the PDP and PCL units of the oligomers and their percentages and the total molecular weights including the TMP initiator. The number-average molecular weight of the oligomer slightly decreased when the amount of depsipeptide increased,

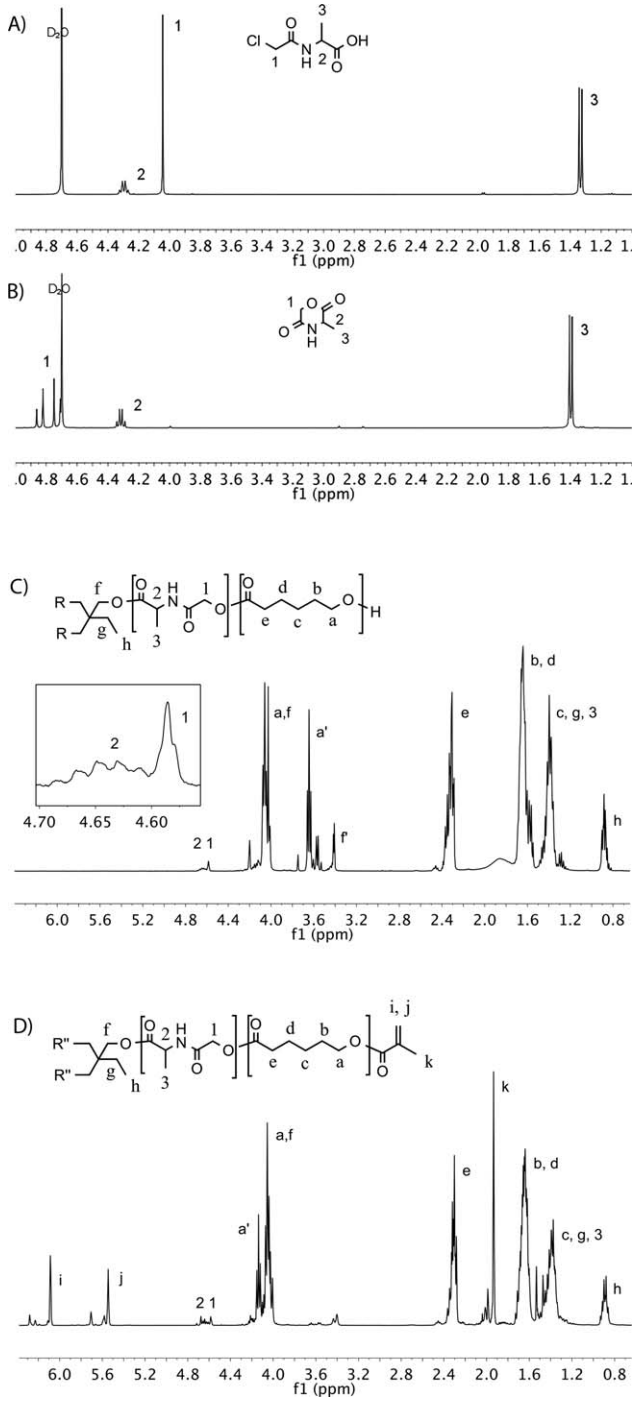

FIGURE 1 ^{1}H NMR spectrum of (**A**) *N*-chloroacetyl-L-alanine in D_2O, (**B**) MMD in D_2O, (**C**) PDP5 oligomer in $CDCl_3$, and (**D**) methacrylated PDP5 macromer in $CDCl_3$.

suggesting that the MMD monomers had a slightly lower reactivity than the CL monomers. Table 1 shows also the molecular weights and polydispersion indexes (PDIs) of the oligomers measured by GPC. Due to a relative nature of the GPC calibration, the values obtained from GPC were consistently higher than the ones calculated from ^{1}H NMR. However, the similarity of the molecular weights of all the oligomers and their narrow molecular weight distributions indicated the successful ROP of all the star-shaped oligomers regardless of the amount of MMD monomer in the synthesis.

To support the ^{1}H NMR data, FTIR was used to characterize the relative amount of amide groups in the resulting photocrosslinkable macromers. Figure 2 shows a decrease in FTIR transmittance near 1540 1/cm when the amount of MMD monomer in the macromer increased. The decreased transmittance is attributed to the increased amount of peptide bonds in the macromer, thus revealing the successful introduction of MMD monomer into the copolymers. This FTIR data is consistent with the data derived from the ^{1}H NMR integrals. FTIR data together with the ^{1}H NMR data thus confirmed that the designated photocrosslinkable copolymers were successfully synthesized.

Thermal Properties of the Oligomers and Macromers

Thermal properties of the oligomers and macromers were characterized with DSC. No melting peaks were detected during the melting run, revealing that all of the oligomers and macromers were amorphous. Figure 3 shows the glass transition temperatures of the oligomers and macromers. It was observed that an increasing amount of MMD in the polymer linearly increased the T_g value, whereas methacrylation did not significantly change the T_g values of the oligomers compared with the macromers. The increase of T_g with the MMD content suggested that the depsipeptides rendered the structures of the copolymers more rigid when compared with the PCL homopolymer. The amorphous nature of the macromers was mainly due to their low molecular weight, which was necessary to ensure that the macromers had low viscosities. All of the methacrylated macromers, as well as the oligomers, were liquids at room temperature. The liquid state of the macromers was highly desired, as it allowed them later to be processed in stereolithography without use of extra heat or solvents.

Double Bond Conversion of the Macromers

The double bond conversion of the macromers during photocrosslinking was evaluated with FTIR. Figure 4 shows the transmittance of the methacrylate double bonds near 1640 1/cm. Before photocrosslinking, the peaks in transmittance curves were observed due to the unreacted double bonds. After photocrosslinking, the peaks disappeared indicating that the double bonds were successfully reacted within 2 minutes of photocrosslinking. To support the FTIR data, gel contents of the photocrosslinked networks were measured, revealing them to be as high as 99.8% $\pm$ 0.1%, 99.2% $\pm$ 0.3%, and 98.3% $\pm$ 0.3% for the PCL, PDP5, and PDP10 samples, respectively. The FTIR data and the high gel contents thus confirmed that the resulting polymer networks were highly crosslinked and the amount of unreacted double bonds of the polymers was very low after photocrosslinking.

In Vitro Biodegradation

The *in vitro* hydrolytic degradation of the photocrosslinked polymers was measured by following the mass loss of the polymer films in PBS. Due to the hydrophobic nature of the photocrosslinked films, the swelling of the samples was minimal and the

TABLE 1 Molecular Weights of the Oligomers (g/mol)

Name	M_n[a] PDP	M_n[a] PCL	M_n[a] ratio (%/%)	M_n[a] total	M_n[b]	PDI[b]
PCL	0	607	0/100	741	1,325	1.25
PDP5	28	576	5/95	738	1,310	1.29
PDP10	49	548	8/92	731	1,303	1.31

[a] Calculated from ^{1}H NMR.
[b] Measured by GPC.

degradation was slow. Figure 5 shows that within 6 months in PBS, the PCL and PDP5 samples lost approximately 8% of their initial mass, whereas the PDP10 samples lost over 15%. To explain the difference in the mass loss, water contact angles of the polymer films were measured, revealing that the photocrosslinked PDP10 films were initially less hydrophobic (contact angle 75° ± 1°, $n = 3$) compared with the PDP5 films (85° ± 1°, $n = 3$) and PCL films (87° ± 1°, $n = 3$). The more hydrophilic surface and the slightly lower gel content of the PDP10 samples thus contributed to their increased mass loss in an aqueous environment compared with the PCL and PDP5 samples. After an initial mass loss attributed to the release of uncured resin to the medium, the degradation rate of the polymer films was constant during the hydrolysis study. The linear mass loss and the intact shape of the films observed during the study indicated that the degradation occurred though surface erosion. This feature suggests that the polymers might later find use especially in zero order drug release applications.

Cytocompatibility of the Photocrosslinked Polymer Films

In vitro cytocompatibility of the photocrosslinked polymers was assessed by measuring the metabolic activity of HUVECs on the polymer films using the colorimetric MTT assay. Figure 6 shows that the optical density, which is proportional to the metabolic activity and number of living cells, increased at every time point within 7 days of cell culturing. At day 7, the optical density was around 10-fold compared with the value at day 1, indicating that the cells proliferated well on the polymer films. The increased metabolic activity of the cells thus showed great cytocompatibility of the photocrosslinked polymers *in vitro*.

Proliferation and Osteogenic Differentiation of C3H10T1/2 Cells on the Films

Mouse pluripotent C3H10T1/2 cells were cultured on the photocrosslinked films to further test the suitability of the

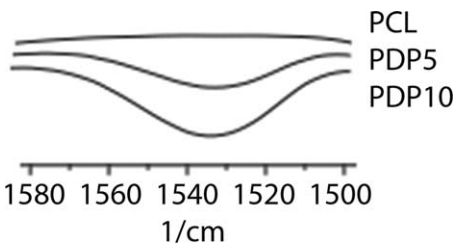

FIGURE 2 FTIR transmittance curves attributed to the peptide bonds of the macromers.

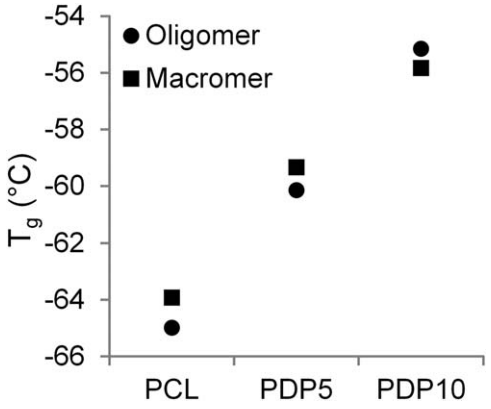

FIGURE 3 Glass transition temperatures of the oligomers and the methacrylated macromers.

polymers for bone tissue engineering. Proliferation of the cells was assessed by measuring the amount of dsDNA within 14 days of cell culturing. Figure 7(A) shows that all of the samples showed greater than a two-fold increase in the amount of dsDNA between day 3 and day 14. The increased amounts of dsDNA indicated that mouse C3H10T1/2 cells proliferated well on the photocrosslinked polymers during 14 days of culturing. The ALP specific activity of the C3H10T1/2 cells was used to indicate the early osteogenic differentiation of the cells. Figure 7(B) shows that the ALP activity was low within 7 days of cell culturing until it increased remarkably before day 14. It has previously been shown that C3H10T1/2 cells have the potential to differentiate into osteoblastic cells.[29,30] In our study, the increased ALP activity suggested that the cells differentiated into osteoblasts on the polymer films within 14 days, thus implying the suitability of these materials for bone applications. The fact that the ALP activity was relatively low at day 7, but higher at day 14, is consistent with the proliferation

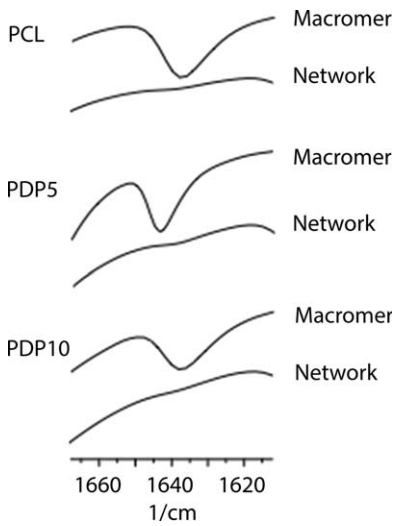

FIGURE 4 FTIR transmittance curves attributed to the methacrylate double bonds before photocrosslinking (Macromer) and after photocrosslinking (Network).

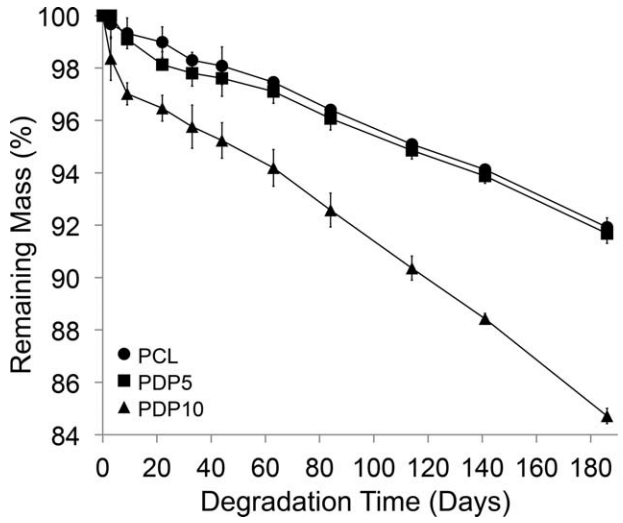

FIGURE 5 Mass loss of the photocrosslinked polymers in PBS.

rate evidenced by the dsDNA concentrations at day 7 and 14, suggesting that the cells first reached confluence and then experienced improved osteogenic differentiation between day 7 and 14.

Preparation of the Photocrosslinked Scaffolds

Stereolithography was used for the preparation of 3D modeled tissue engineering scaffolds. The photocrosslinkable resin containing macromer and photoinitiator showed a desired viscosity at room temperature and no solvents or heating was required. Addition of a small amount of orange dye into the polymer resin was needed to prevent overcuring that otherwise would affect the pore size and geometry of the scaffold during the building process. The fabrication of the scaffolds proceeded well for all of the macromers, and no changes to the fabrication parameters were needed for different resins. No shrinkage of the photocrosslinked materials was observed after solvent extraction, and the final dimensions of the scaffolds were as designed. Figure 8(A) shows that the color of the scaffolds varied from light yellow (PCL) to orange (PDP10), which is attributed to the increasing amount of depsipeptide in the polymer causing an increasingly yellow color. The SEM picture in Figure 8(B) shows that the pore architecture of the scaffolds was in a repeated gyroid pattern as designed in our 3D model.

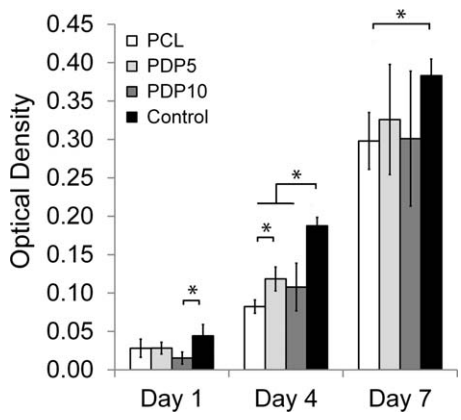

FIGURE 6 Metabolic activity of HUVECs cultured on the photocrosslinked films and on a TCPS control.

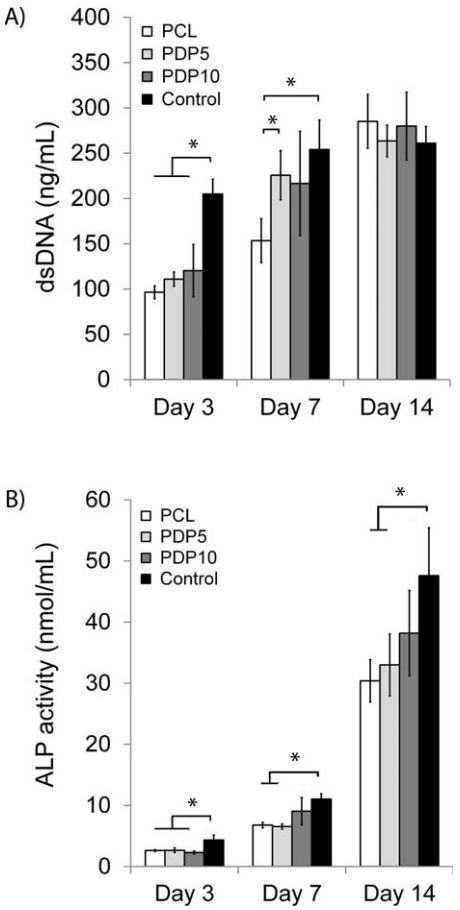

FIGURE 7 (**A**) Cellular dsDNA content and (**B**) ALP activity of C3H10T1/2 cells cultured on the photocrosslinked films and on a TCPS control.

Mechanical Properties of the 3D Scaffolds

The effect of depsipeptide on the mechanical properties of the scaffolds was measured with compressive strength tests. All of the scaffolds showed a long linear stress–strain curve before yielding, thus indicating the elasticity of the materials (the curves are shown in the Supporting Information). Figure 9(A–D) shows the load and strain at the yield point and the stiffness and the compression modulus of the scaffolds calculated using the strain range of 0%–10%. No statistically significant difference was observed between the properties of the PCL and PDP5 scaffolds. However, 10 mol % of MMD, as in PDP10, was sufficient to increase the values significantly. The PDP10 scaffolds had a three-fold higher load and a two-fold higher strain at the yield point when compared with the PCL scaffolds. Additionally, the compression modulus and stiffness were significantly higher for the PDP10 scaffolds than for the other scaffolds. The increased mechanical strength of the PDP10 scaffolds can be attributed to the fact that L-alanine molecules in the depsipeptide units can form

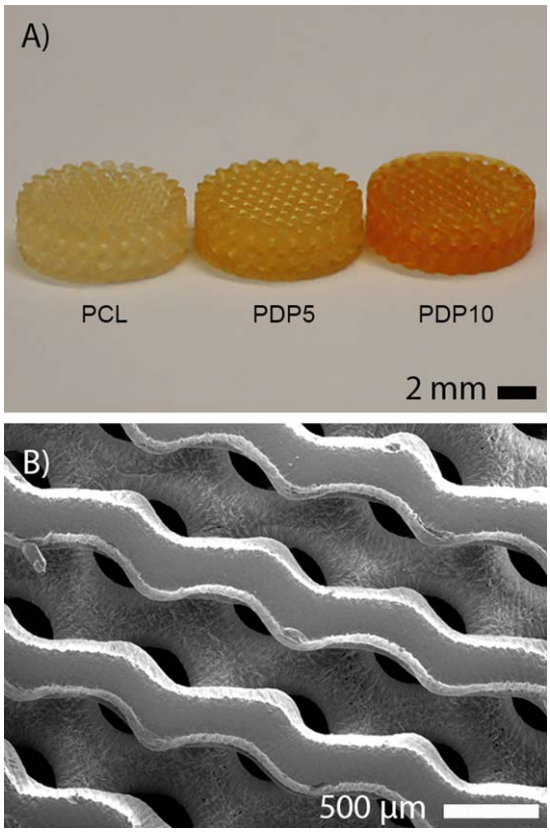

FIGURE 8 (**A**) Photograph of the scaffolds prepared by stereolithography and (**B**) SEM image of the top surface of the PDP10 scaffold.

strong intermolecular hydrogen bond interactions between the amide groups,[15] enhancing the mechanical strength of the resulting scaffolds. Apparently, 5 mol % MMD was not sufficient to significantly change the mechanical properties of the PDP5 scaffolds when compared with the PCL scaffolds.

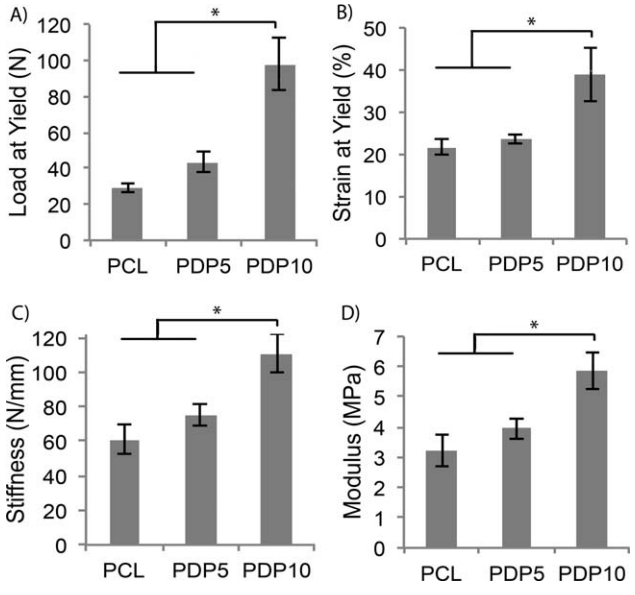

FIGURE 9 (**A**) Maximum load at the yield point, (**B**) strain at the yield point, (**C**) stiffness, and (**D**) compression modulus of the scaffolds prepared by stereolithography.

CONCLUSIONS

In this study, we reported the synthesis of a new type of photocrosslinkable poly(ester amide) which can be used for 3D photofabrication of tissue engineering scaffolds. Star-shaped copolymers based on CL and L-alanine-derived depsipeptide were successfully synthesized, and the new polymers were processed into mathematically defined porous scaffolds by stereolithography. The incorporation of depsipeptide into PCL increased the glass transition temperature of the polymer, suggesting a more rigid nature of the poly(ester amide) copolymer compared with the PCL homopolymer. The hydrolytic degradation of the photocrosslinked copolymer increased when compared with the homopolymer, partly resulting from the more hydrophilic nature of the copolymer. Also the compressive strength of the 3D scaffolds increased with the increasing depsipeptide content, which we suggested to result from the strong intermolecular interactions between the amide groups. *In vitro* cell studies showed excellent cytocompatibility of the photocrosslinked polymers. The results in this study suggested that our new photocrosslinkable poly(ester amide) copolymer, which can be tailored by changing the amino acid in the monomer, is promising material for photofabrication of high-resolution tissue engineering scaffolds. In the future, further studies are needed to evaluate the biodegradation and biocompatibility of the polymer under *in vivo* conditions.

ACKNOWLEDGMENTS

Graduate School in Chemical Engineering (LE), the American-Scandinavian Foundation (LE), Finnish Foundation for Technology Promotion (LE), the Research Foundation of Helsinki University of Technology (LE), NIH R01AR057837 (NIAMS, YY), NIH R01DE021468 (NIDCR, YY), DOD W81XWH-10-1-0966 (PRORP, YY), and Coulter Translational Research Award (YY) are gratefully acknowledged for the funding. Anthony Behn (Stanford University) is acknowledged for his help with the mechanical testing and Colin McKinlay (Stanford University) for running the GPC analysis of our polymers.

REFERENCES AND NOTES

1 F. B. W. Melchels, J. Feijen, D. W. Grijpma, *Biomaterials* **2010**, *31*, 6121–6130.

2 H. Lin, D. Zhang, P. G. Alexander, G. Yang, J. Tan, A. W. M. Cheng, R. S. Tuan, *Biomaterials* **2013**, *34*, 331–339.

3 K. S. Anseth, D. J. Quick, *Macromol. Rapid Commun.* **2001**, *22*, 564–572.

4 F. P. W. Melchels, J. Feijen, D. W. Grijpma, *Biomaterials* **2009**, *30*, 3801–3809.

5 J. Jansen, F. P. W. Melchels, D. W. Grijmpa, J. Feijen, *Biomacromolecules* **2009**, *10*, 214–220.

6 B. G. Amsden, G. Misra, F. Gu, H. M. Younes, *Biomacromolecules* **2004**, *5*, 2479–2486.

7 L. Elomaa, S. Teixeira, R. Hakala, H. Korhonen, D. W. Grijpma, J. V. Seppälä, *Acta Biomater.* **2011**, *7*, 3850–3856.

8 L. Cai, S. Wang, *Polymer* **2010**, *51*, 164–177.

9 L. Elomaa, A. Kokkari, T. Närhi, J. V. Seppälä, *Compos. Sci. Technol.* **2013**, *74*, 99–106.

10 S. Schüller-Ravoo, J. Feijen, D. W. Grijpma, *Macromol. Biosci.* **2011**, *11*, 1662–1671.

11 K.-W. Lee, S. Wang, B. C. Fox, E. L. Ritman, M. J. Yaszemski, L. Lu, *Biomacromolecules* **2007**, *8*, 1077–1084.

12 M. Vert, *Biomacromolecules* **2005**, *6*, 538–546.

13 H. Sun, F. Meng, A. A. Dias, M. Hendriks, J. Feijen, Z. Zhong, *Biomacromolecules* **2011**, *12*, 1937–1955.

14 W. Khan, S. Muthupandian, S. Farah, N. Kumar, A. J. Domb, *Macromol. Biosci.* **2011**, *11*, 1625–1636.

15 Y. Feng, J. Lu, M. Behl, A. Lendlein, *Macromol. Biosci.* **2010**, *10*, 1008–1021.

16 Y. Feng, J. Guo, *Int. J. Mol. Sci.* **2009**, *10*, 589–615.

17 P. J. Dijkstra, J. Feijen, *Macromol. Symp.* **2000**, *153*, 67–76.

18 Y. Feng, C. Chen, L. Zhang, H. Tian, W. Yuan, *Trans. Tianjin Univ.* **2012**, *18*, 315–319.

19 T. Ouchi, H. Seike, T. Nozaki, Y. Ohya, J. *Polym. Sci., Part A: Polym. Chem.* **1998**, *36*, 1283–1290.

20 D. A. Barrera, E. Zylstra, P. T. Landsbury, R. Langer, *Macromolecules* **1995**, *28*, 425–432.

21 J. Helder, F. E. Kohn, S. Sato, J. W. Berg, J. Feijen, *Makromol. Chem., Rapid Commun.* **1985**, *6*, 9–14.

22 Y. Ohya, T. Nakai, K. Nagahama, T. Ouchi, S. Tanaka, K. Kato, *J. Bioact. Compat. Polym.* **2006**, *21*, 557–577.

23 A. Battig, B. Hiebl, Y. Feng, A. Lendlein, M. Behl, *Clin. Hemorheol. Micro.* **2011**, *48*, 161–172.

24 Y. Zhao, J. Li, H. Yu, G. Wang, W. Liu, *Int. J. Pharm.* **2012**, *430*, 282–291.

25 G. John, S. Tsuda, M. Morita, *J. Polym. Sci., Part A: Polym. Chem.* **1997**, *35*, 1901–1907.

26 C. A. Reznikoff, D. W. Brankow, C. Heidelberg, *Cancer Res.* **1973**, *33*, 3231–3238.

27 F.-N. Fung, R. C. Glowaky, U.S. Patent 4916209, April 10, 1990.

28 T. Jiang, W. I. Abdel-Fattah, C. T. Laurencin, *Biomaterials* **2006**, *27*, 4894–4903.

29 Katagiri, A. Yamaguchi, T. Ikeda, S. Yoshiki, J. M. Wozney, V. Rosen, E. A. Wang, H. Tanaka, S. Omura, T. Suda, *Biochem. Biophys. Res. Commun.* **1990**, *172*, 295–299.

30 G. Bain, T. Müller, X. Wang, J. Papkoff, *Biochem. Biophys. Res. Commun.* **2003**, *301*, 84–91.